



EXPERIMENTAL STUDY ON THE SEISMIC BEHAVIOR OF A NOVEL TYPE OF ALL-STEEL BUCKLING- RESTRAINED BRACES

Junxian Zhao¹, Bin Wu² and Jinping Ou^{2,3}

ABSTRACT

To minimize the residual welding deformation in the steel core with cruciform cross-section of conventional all-steel buckling-restrained braces (BRBs), a novel all-steel BRB, called angle steel BRB (ABRB), has been developed. The steel core of ABRB consists of four angle steels with equal sides to form a non-welding cruciform cross-section as the energy dissipation part. The outer restraint is composed of two angle steels with equal sides welded longitudinally to form a square hollow cross-section. The component test including three ABRB specimens under quasi-static cyclic load was conducted to investigate the effects of the boundary condition, the brace end rotation demand and the constructional details in the steel core segment on the seismic behavior of ABRBs. The test results indicate that the ABRB specimen with rigid connection exhibits superior seismic performance than the others. The local compression-flexure failure occurs at the core projection for the hinge connected specimen without any rotation restraint, but such failure mode can be safely prevented by providing rotation restraint at the brace end. The stopper with the abrupt change of the cross-section in the middle of the steel core induces stress concentration and impair its low-cycle fatigue property. Finally, the seismic performance of the ABRB specimens is analyzed, which shows that the seismic performance parameters of the ABRBs well satisfy the requirement specified by the AISC seismic provision, so the ABRB can serve as an effective passive energy dissipation device for engineering structures.

Introduction

Buckling-restrained braces (BRB) are both lateral bracing and seismic control members, which consist of an inner steel core and an outer restraint. Due to the restraining effect by the outer part, the steel core can yield both in tension and compression without buckling and dissipate much seismic energy.

¹PhD Candidate, School of Civil Engineering, Harbin Institute of Technology, Harbin 150090, China

²Professor, School of Civil Engineering, Harbin Institute of Technology, Harbin 150090, China

³Professor, School of Civil and Hydraulic Engineering, Dalian University of Technology, Dalian 116024, China

The all-steel BRBs, of which the steel core is restrained by all-steel components, have gained wide acceptance mainly in Japan and China because of their light weight and easy assembly. The conventional all-steel BRBs are illustrated in Figure 1, of which the steel core consists of cruciform cross-section welded by three steel plates. Investigations on the seismic behavior of all-steel BRB have been conducted by many researchers: The tests by Koetaka (Koetaka 2000), Fukuda (Fukuda 2004) and Ma (Ma 2008) showed that significant amount of welding in the yielding segment of steel core would impair the low-cycle fatigue property of the core. Furthermore, the tests by Ma (Ma 2008) also revealed that the actual yielding force of the all-steel BRB illustrated in Figure 1(a) was significantly affected by the high temperature welding and the additional cross-section area of the welding, which make it difficult to predict the actual performance of such all-steel BRB. Murase (Murase 2004) found that the residual welding deformation in the steel core would make it difficult to assemble.

To minimize the residual welding deformation in the steel core with cruciform cross-section and enhance the seismic performance of conventional BRBs, a novel type of all-steel BRB, called angle steel BRB (ABRB), has been developed. As is depicted in Figure 2, the steel core of ABRB consists of four angle steels with equal sides to form a non-welding cruciform cross-section. The outer restraint is composed of two angle steels with equal sides welded longitudinally to form a square hollow cross-section.

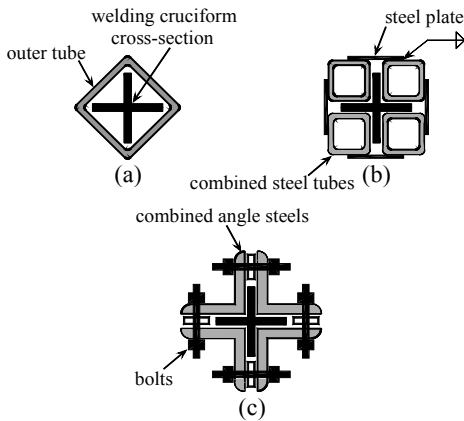


Figure 1. Conventional all-steel BRBs

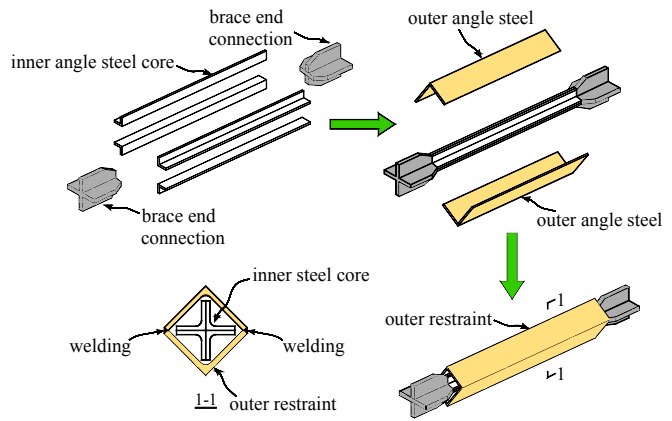


Figure 2. Angle steel BRB

This paper will describe the component test on three ABRB specimens under uniaxial quasi-static cyclic load to investigate the effects of the boundary condition, the rotation demand at the brace end and the constructional details in the steel core segment on the seismic behavior of ABRBs.

Test Program

Test specimens

Three ABRB specimens with different configurations were designed. Figure 3 and Figure 4 illustrate the configuration of the inner steel cores and the entire ABRB specimens with outer restraint respectively. The detailed specimen parameters are presented in Table 1. The yield

force P_{yc} is calculated by multiplying the yield stress obtained from the tensile coupon tests by the cross-sectional area of the yielding segment A_y ; the Euler buckling load of the outer restraint P_e is calculated based on the length of the outer angle steels (L). The yield displacement δ_{yc} corresponds to the axial deformation of the steel core when the axial force reaches P_{yc} . A_1 represents the cross-sectional area of the core projection.

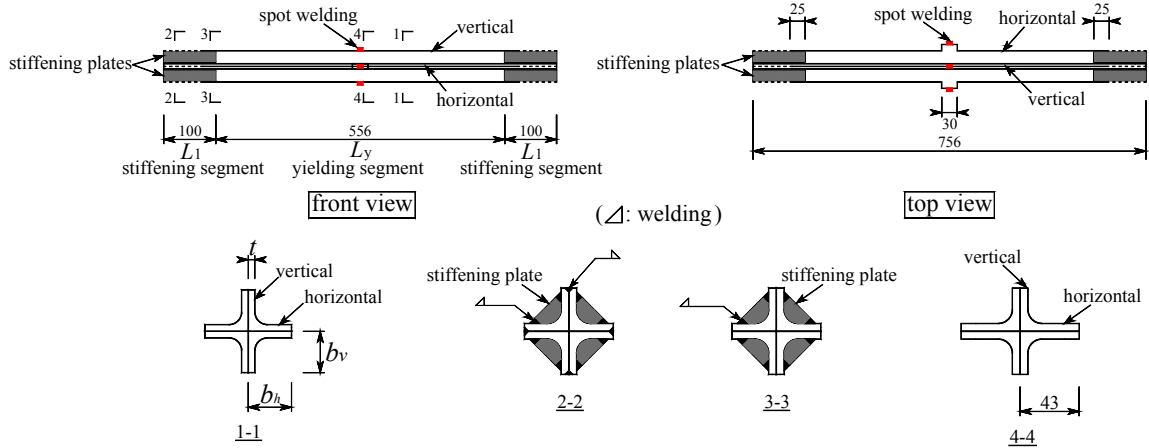


Figure 3. Configuration of the inner steel core specimens

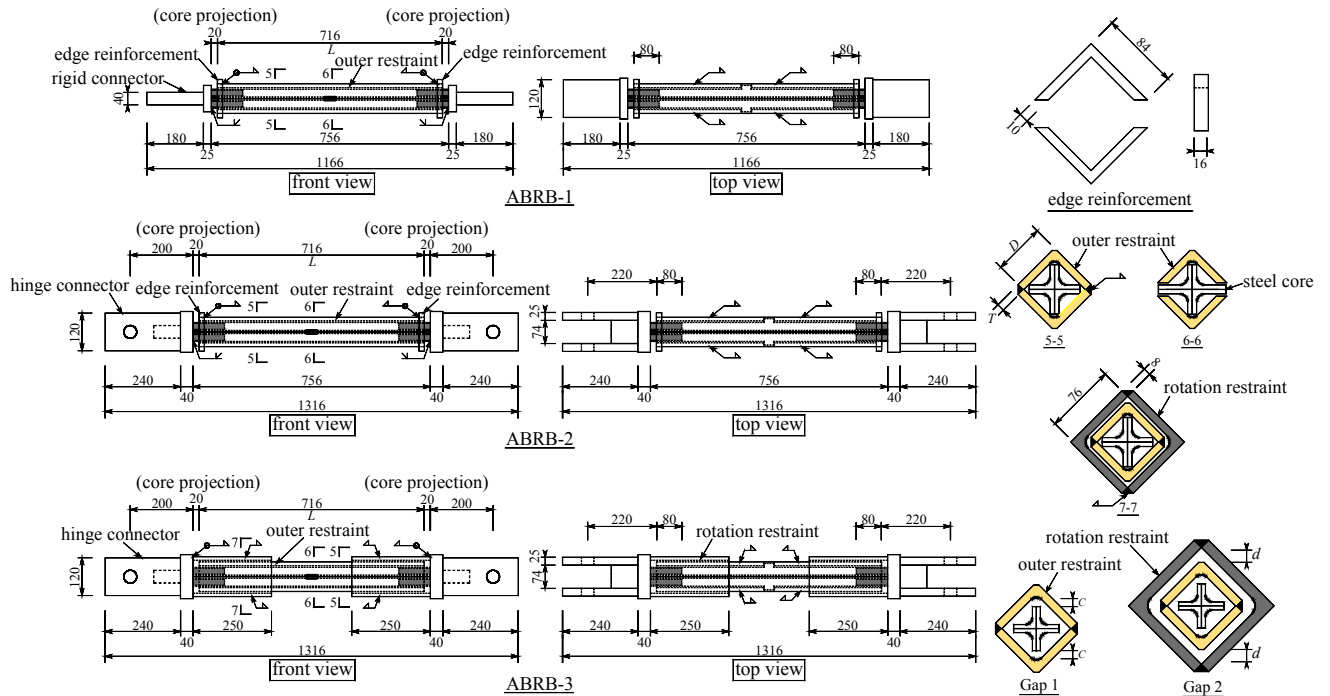


Figure 4. Configuration of the ABRB specimens

Table 1. Detailed parameters of the ABRB specimens

Specimen	Boundary condition	Inner steel core								Outer restraint				ABRB
		L_1 (mm)	L_y (mm)	b_h (mm)	b_v (mm)	t (mm)	A_1/A_y	δ_{yc} (mm)	P_{yc} (kN)	D (mm)	T (mm)	c (mm)	L (mm)	P_e/P_{yc}
ABRB-1	rigid	97	561.7	30.3	29.4	4.72	1.95	1.01	320.3	58.3	7.7	0.93	716.9	12.8
ABRB-2	hinge	98	561	30.3	29.3	4.57	1.98	1.01	310.4	58.2	7.7	1.03	717	13.2
ABRB-3	hinge	97	561.3	30.3	28.9	4.65	1.97	1.01	313.1	58.1	7.7	1.12	716.5	13.1

The individual angle steels were all manufactured by milling machine without any flame cut and the total design length of the steel core was 756 mm for all the specimens. The horizontal limbs of the angle steel cores were locally enlarged in the middle as a stopper to prevent the outer restraint from slipping (Figure 3). The angle steel cores were welded together between the adjacent angle steel limbs within the stiffening segment (The dashed line and section 2-2 in Figure 3) to maintain the integrity of the core projection. Both ends of the steel cores were reinforced by welding four stiffening plates to keep it elastic within the stiffening segment of the core, and a distance of 25 mm was provided between the end of the welding line of the angle steel cores and that of the stiffening plates to avoid the stress concentration induced by residual welding stress. The four angle steels within the steel core were connected together only in the middle by four small spot welding points to ensure machining precision during manufacturing process.

Two kinds of connectors including hinge and rigid connection were designed to investigate the effect of the boundary condition on the seismic behavior of ABRBs. All of the connectors were connected to the corresponding steel core specimens by butt weld.

The outer restraint comprises two angle steels with equal sides welded longitudinally to form a square hollow cross-section (Section 5-5 in Figure 4), and it has a total length of 716 mm for all the specimens, which is 40 mm shorter than that of the steel core to accommodate the relative axial deformation in between. A gap of about 1 mm was provided between the steel core and the outer restraint to accommodate the lateral expansion of the core when it is under compression due to the Poisson's effect. The outer angle steels were locally cut in the middle so as to get themselves stuck by the stoppers in the middle of the steel core (Section 6-6 in Figure 4), hence the axial slippage of the outer restraint can be prevented. Furthermore, both ends of the outer restraint for specimen ABRB-1 and ABRB-2 were reinforced to prevent the local failure at the edge of the outer restraint.

In order to restrict the brace end rotation demand, the rotation restraint was designed for specimen ABRB-3. Such rotation restraints consist of two short angle steels with equal sides welded together to form a square hollow cross-section (Section 7-7 in Figure 4). One end of the rotation restraints was welded to the end plate of the connectors and a gap was also provided between the rotation restraint and the outer restraint. It was mainly designed to restrain the rotation development at the brace end without excessively transmitting the axial load.

Table 2. Mechanical properties of major steel materials

Material	Material grade	Yield stress f_y (MPa)	Tensile strength f_u (MPa)	Yield ratio f_y/f_u	Elastic modulus E (MPa)	Elongation percentage δ (%)
steel core L50×5	Q235-B	301.0	439.5	0.68	1.99×10^5	36.9
Outer restraint L90×8	Q235-B	256.3	412.6	0.62	2.03×10^5	36.3
Stiffening plate	Q345-B	364.2	535.4	0.68	2.13×10^5	27

The Chinese structural steel Q235-B with nominal yield stress of 235 MPa was used for the inner steel core, the outer restraint and the rotation restraint. The stiffening plate steel was grade Q345-B with nominal yield stress of 345 MPa. The mechanical properties of the major steel materials obtained from tensile coupon tests are listed in Table 2.

Test Setup

The component tests were conducted under quasi-static cyclic load on the MTS electro hydraulic test machine with maximum axial force of 2500 kN in the Structural and Seismic Testing Center at the Harbin Institute of Technology, China. The test setup is shown in Figure 5.



Figure 5. Test setup

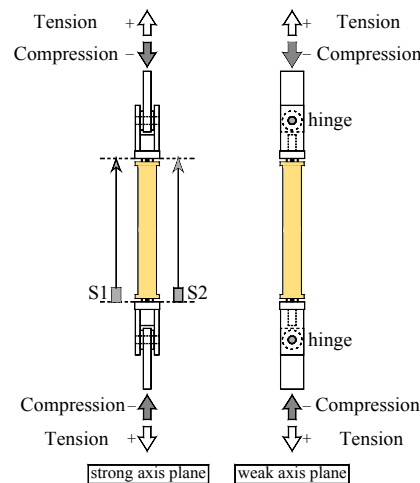


Figure 6. Arrangement of displacement transducers

As is shown in Figure 6, two displacement transducers (string potentiometers) labeled S1 and S2 were mounted between the two end plates of the connectors within the strong axis plane. The mounting points were located at the ends of the steel core to measure the axial deformation of the steel core itself (not including the deformation of the connectors). The axial force of the specimens were measured by the load cell of the MTS actuator.

Loading Protocol

As is shown in Table 3, uniaxial quasi-static cyclic loading protocol was applied under

displacement controlled mode of actuator, in which the loading was imposed at the target steel core strain amplitude of 0.4%, 0.6%, 0.8%, 1.0%, 1.2%, 1.4%, 1.6%, 1.8%, 2.0%, 2.2%, 2.6% and 3.0% until the specimen failed. All the loading cycles began with compression and two cycles were adopted for each of the strain amplitude except for the six loading cycles at the strain amplitude of 1.4% to investigate the strength and stiffness degradation.

Table 3. Loading protocol

Loading sequence	Target axial strain (%)	Loading cycles	Target axial deformation (mm)
1	0.4	2	2.25
2	0.6	2	3.37
3	0.8	2	4.49
4	1	2	5.62
5	1.2	2	6.74
6	1.4	6	7.86
7	1.6	2	8.98
8	1.8	2	10.11
9	2	2	11.23
10	2.2	2	12.35
11	2.6	2	14.60
12	3	—	16.85

Test Result and Analysis

The relationship between the nondimensional axial load P/P_{yc} and the axial strain ϵ of the steel core (average axial deformation measured by the string potentiometers divided by the actual length of the yielding segment L_y) are illustrated in Figure 7 (positive in tension and negative in compression), in which the shadowed triangle denotes the starting point of the strength degradation, indicating the specimen failure. The detailed seismic performance parameters are shown in Table 4, in which the subscript t and c denote the tension and the compression respectively, and the tension strength adjustment factor ω denotes the maximum tension force T_{max} divided by the computed yielding axial force P_{yc} (computed from the tensile coupon test). As can be seen, after the braces yield, all the specimens exhibit plump and stable hysteretic performance without visible strength or stiffness degradation before specimen failure, and the maximum ductility μ , the cumulative inelastic axial ductility η and the compression strength adjustment factor β have all met the requirement ($\mu \geq 10$, $\eta \geq 200$, $\beta \leq 1.3$) specified in the AISC Seismic Provision (AISC 2005), which indicate that the ABRBs exhibit satisfactory hysteretic energy absorption capacity and can serve as an effective energy dissipation device for engineering structures.

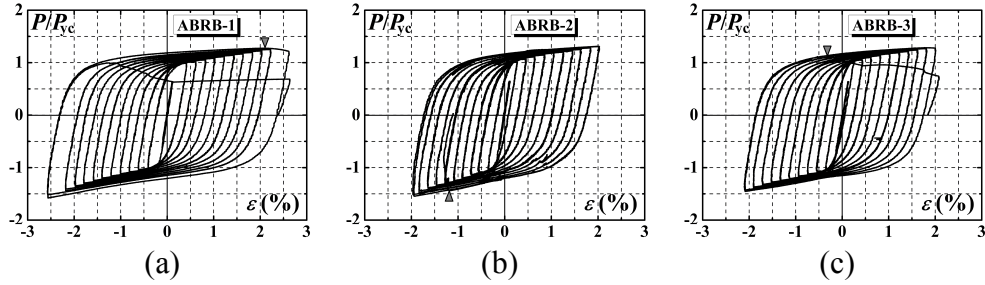








Figure 7. Hysteretic curves of the ABRB specimens

Table 4. Major seismic performance parameters of the ABRB specimens

Specimen	ω	β	ε_t (%)	ε_c (%)	μ_t	μ_c	η
ABRB-1	1.26	1.14	2.24	-2.57	12.1	14.3	646
ABRB-2	1.30	1.18	2.04	-1.98	11.4	11.1	539.8
ABRB-3	1.29	1.10	2.02	-2.12	11.3	11.8	518

Table 5. Failure modes of the ABRB specimens

Specimen	Final overall failure mode	Final local failure mode	Description of the failure mode
ABRB-1			Some of the angle steel cores ruptured at the tensile axial strain of 2.1% during the first 2.6% tension excursion
ABRB-2			Local compression-flexure failure occurred at the core projection at the compressive axial strain of -1.2% during the second 2% compression excursion
ABRB-3			Some of the angle steel cores ruptured at the axial strain of -0.3% during the second 2% from the compression to tension excursion

As is shown in Figure 7 and Table 5, the boundary condition, the rotation demand at the brace end and the constructional details in the yielding segment of the steel core are three major influential factors on the seismic behavior of the ABRBs. The local compression-flexure failure was prone to occur at the core projection for the hinge connected ABRB specimen without rotation restraint at the brace ends, and such failure mode could be safely prevented for the hinge connected ABRB specimen with rotation restraint and the ABRB specimen with rigid connections. For the hinge connected ABRB without rotation restraint, the brace end rotation demand θ was much larger than that of the other specimens, resulting in an increase of the value of the loading eccentricity e , so the core projection would be subjected to a combined axial force

P and a bending moment M caused by loading eccentricity simultaneously. It appears that a further discussion will be needed to examine the design method of the core projection for the hinge connected ABRB without rotation restraint. On the other hand, the stoppers with the abrupt change of the cross-section in the middle of the steel core yielding segment resulted in a stress concentration at such location for the specimen ABRB-1 and ABRB-3, which impaired the low-cycle fatigue property and caused an early rupture of the steel core.

Conclusions

A novel all-steel buckling-restrained brace, called angle steel BRB (ABRB), has been developed to minimize the residual welding deformation of the steel core and enable easier assembly of all-steel BRB members. Component test including three ABRB specimens was conducted under uniaxial quasi-static cyclic load and the effects of the boundary condition, the brace end rotation demand and the constructional details in the steel core yielding segment were investigated. The main conclusions are summarized as follows:

(1) The proposed ABRBs exhibit plump and stable hysteretic performance with the maximum axial strain of approximately 2.6% and the maximum cumulative inelastic axial ductility η of 646, which has far exceeded the lower limit specified by the AISC seismic provisions, so it can be concluded that the ABRB can serve as an effective energy dissipation device for engineering structures.

(2) To prevent the early local compression-flexure failure at the core projection, it is suggested the brace end rotation should be restrained by the rotation restraint or rigid connections at the brace end.

(3) The stopper with the abrupt change of the cross-section in the middle of the steel core yielding segment will impair the low-cycle fatigue property of the core and it should be improved by the gradual change of the cross-section to minimize the stress concentration.

Acknowledgments

The project was supported by the National Basic Research Program of China (973 Program) (2007CB714204) and the National Key Technology R&D Program (2006BAJ03B06-01 and 2006BAJ06B03-03). The authors also would like to express great thanks to Dr. Yubin Tian, Mr. Yunfei Ma and other laboratory personnel at the Structural and Seismic Testing Center, Harbin Institute of Technology, China for their assistance during the tests.

References

- Koetaka, Y., Tsujita, O. and Narihara, H., 2000. *The experimental study on buckling restrained braces (Part 2)*, Summaries of Technical Papers of Annual Meeting, Architectural Institute of Japan, 913-914. (in Japanese)
- Fukuda, K., Makino, T. and Ichinohe, Y., 2004. *Development of brace-type hysteretic dampers*, Summaries of Technical Papers of Annual Meeting, Architectural Institute of Japan, 867-868. (in Japanese)
- Ma, N., Zhao, J.X., Wu, B., et al, 2008. *Full scale subassembly test of all-steel buckling restrained*

- brace*, Proceeding of the Tenth International Symposium on Structural Engineering for Young Experts, Beijing, China, 949-954.
- Murase, Y., Morishita, K., Inoue, K., et al, 2004. *Structural design method of the long brace with axial hysteresis dampers at both ends (Part 1)*, Journal of Structural and Construction Engineering, 578(4), 131-138. (in Japanese)
- ANSI/AISC 341-05, 2005. *Seismic Provisions for Structural Steel Buildings*, American Institute of Steel Construction, Chicago, Illinois.